[redacted]

Cosmic Ray Physics Report

LUIP-CR-74-07

August 1974

EXPERIMENTAL AND THEORETICAL ABSORPTANCE PROFILES OF TRACKS OF FAST HEAVY IONS IN NUCLEAR EMULSION

M. Jensen, L. Larsson, O. Mathiesen and R. Rosander

Department of Physics

University of Lund

Sölvegatan 14

S-223 62 LUND, Sweden

EXPERIMENTAL AND THEORETICAL ABSORPTANCE PROFILES OF TRACKS OF FAST HEAVY IONS IN NUCLEAR EMULSION

M. Jensen, L. Larsson, O. Mathiesen and R. Rosander

CONTENTS

EXPERIMENTAL AND THEORETICAL ABSORPTANCE PROFILES OF TRACKS OF FAST HEAVY IONS IN NUCLEAR EMULSION

M. Jensen, L. Larsson, O. Mathiesen and R. Rosander
Department of Physics, University of Lund, Lund, Sweden

ABSTRACT

Transverse absorptance profiles of 27 tracks of cosmic ray nuclei recorded in Ilford G5 nuclear emulsion have been measured by a nuclear track photometer. Included in the study were nuclei with atomic numbers 14, 16, 20, 24 and 26 with velocities relative to that of light within the interval $0{,}3 \leq \beta \leq 0.8$. The experimental absorptance profiles have been compared with theoretical profiles calculated from the δ-ray theory of track formation developed by Katz and coworkers. Taking into account the re-scattering of light into the cone of acceptance of the photometer, good agreement has been found between experimental and theoretical profiles within the entire charge and velocity interval. The semi-empirical formula for high aperture photometry is discussed in some detail, as well as the theory of δ-ray production and the transport of electrons and their energy dissipation in nuclear emulsion.

1. INTRODUCTION

A detailed knowledge of the process by which the kinetic energy of a fast heavy ion is deposited in an absorber is of great interest in a variety of fields in physics, biology and medicine. For instance, when working with nuclear emulsions as in the present study, such a knowledge, as manifested by a reliable theory of track formation, can be expected to bring the assignment of the charge number and velocity to the recorded particles to a higher accuracy than obtainable by simple interpolation or extrapolation in the experimental data. In this field a successful theory would also make it feasible to interrelate the results obtained for different experimental conditions, e.g. using the same stack of emulsion but different techniques or vice versa.

The spatial region around the path of the ion which must be taken into account in a track formation theory may vary considerably from one experiment to the other. At the one extreme the attention may be focused only on the structure of the track core, i.e. the volume along the track axis characterized by the diameter of an AgBr grain. In this region the linear properties of the track, e.g. grain density, can be described by the concept of restricted energy loss (REL), as proposed by Messel and Ritson (1). This concept should in the first place be useful for tracks of particles with low ionization. However, as shown in a previous study by Jensen, Larsson and Rosander (2), REL can also be used for tracks of particles with high ionizing power, provided that a correspondingly higher value is chosen for the maximum energy of the secondary

electrons which are considered in the REL formula.

At the other extreme there are situations where a much larger volume around the track axis has to be considered, e.g. studies of tracks of heavy ions by photometric methods. The radial distances which can be of interest depend on the experimental conditions, but, to orders of magnitude, they are 10 to 100 μm. A theory intended to describe the track structure in this extended spatial region must necessarily take into account the production, propagation and energy loss of all secondary electrons regardless of their energy. A first step towards such a theory was taken by Bizzeti and Della Corte (3). Their model has been revised by Katz and Butts (4), and subsequently amended and modified in a series of papers by Katz and coworkers (5,6,7,8). A current formulation of this theory, referred to as Katz's theory in this paper, can be found in the paper by Katz et al. (9).

In the present paper we compare Katz's theory with experimental measurements of the structure of tracks of heavy ions. The atomic number Z of the ions is in the interval $14 \leq Z \leq 26$ and the ion velocity β relative to that of light in the interval $0.3 \leq \beta \leq 0.8$. The study is based on photometrical measurements of the light transmittance as a function of the lateral distance from the track axis. Such a set of transmittances will in the following be referred to as a transmittance profile. In the next section the relevant experimental details are presented and in Section 3 Katz's theory is outlined. Some of the underlying assumptions are discussed in the Appendix. Section 4 deals with the calculation of the theoretical light transmittance profiles. The results of the comparison of observed and calculated profiles are given in Section 5.

Preliminary results of this study have been reported previously (10,11).

2. EXPERIMENTAL DETAILS

2.1. The detector

The part of the emulsion stack which was used in the present study was composed of 65 Ilford G5 nuclear emulsion sheets, each of them having a thickness of 600 μm and an area of 10 x 20 cm^2. The stack was exposed to the cosmic radiation in a balloon flight from Fort Churchill, Canada, in July 1967. The emulsions were developed by the usual temperature development method. The plateau value of the blob density of singly charged particles was found to be 180 mm^{-1}. Thus the degree of development can be regarded as normal.

2.2. The photometer

The photometer used in the present study has been described by Jacobsson et al. (12). The optical part of the apparatus is shown in Figure 1. We used a 53x oil immersion objective and a two-diaphragm condenser, both with a numerical aperture of 0.95. The angular extension of the actual light cone was slightly reduced by the aperture diaphragm of the condenser to improve the quality of the visual image.

The width and the length of the photometer slit image in the object plane were 0.31 μm and 24.4 μm respectively. In taking the readings the image of the track segment was first adjusted parallel to the slit. Then the image was swept across the slit in a direction perpendicular to the track axis.

2.3. The selection of tracks

Only tracks of stopping particles were used in the present

study. The tracks were selected from a larger set analysed by Söderström et al. (13). The charge number of the particles was determined by these authors. They estimate the uncertainty in the charge assignment to be about 0.3 units of charge. The ion velocity was obtained from the known residual range and the charge number Z.

In order to minimize the systematic errros due to differences in dip angle and due to the possible existence of processing gradients over the volume of the pellicles, as well as differences in light scattering at different depths in the emulsion, all tracks accepted in the present study had to fulfil the following criteria.

1. The tangent of the dip angle in the unprocessed emulsion must be less than 0.35.
2. The track must be situated more than 8 mm from all edges of the pellicle.
3. No readings must be taken outside the depth interval from 30 % to 55 % of the emulsion thickness, the reference level being the air surface of the pellicle.

The number of accepted tracks at different values of Z and β is shown in Table I.

2.4. The measurements

All experimental transmittance profiles have been based on readings of the radiant flux of light in 24.4 μm long sections of the track, the length being dictated by the length dimension of the image of the photometer slit in the object plane. For reference purposes it is convenient to define a Cartesian coordinate system (x,y,z) with its origin in the centre of the track segment, x-axis along the projection of the track in the emulsion plane, and positive z-axis coinciding with

the positive normal to the surface of the pellicle.

Each transmittance profile has been based on readings of the photomultiplier current taken at 1 μm intervals out to a lateral distance $y \simeq \pm 85$ μm. Due to differences in the general transmittance level of different plates and variations of the transmittance with the depth in the emulsion, the photomultiplier signals must be normalized. This was effected by assigning a transmittance of unity to the average value of the 15 outermost readings on both flanks of the profile. At such distances the grain density due to the track is negligible. In the parallel beam approximation discussed in Section 4.1 the contribution of a constant absorptance due to background grains becomes a multiplying factor to the transmittance profile. Thus in this approximation our normalizing procedure should eliminate the effect of background grains and the normalized transmittance profile should be directly comparable with a profile calculated for a backgroundless emulsion. Possible nonlinear effects of the background resulting from the large angular extent of the light cone are discussed in Section 5.2.

In order to reduce the random fluctuations, four profiles were taken for each track specified by a given combination of Z and β in Table I. The four profiles were taken at somewhat different residual range but so close together that the β-dependence of the profiles with sufficient accuracy could be assumed to be linear. The residual ranges were chosen such that the average velocity for each set of four profiles coincided with the β value quoted in Table I.

2.5. Data reduction and smoothing

For numerical reasons all data points, about 84,000 in number, could not be used in the comparison with the theory and

therefore the data had to be condensed. In addition to the smoothing obtained by taking averages, specific smoothing procedures were applied to suppress the influence of random fluctuations which otherwise would complicate the comparison with theory. The course of action has been the following.

For each combination of Z and β an average transmittance profile was determined. An analytical form for the average profile was obtained by fitting a fifth degree polynomial to the logarithms of transmittance and lateral distance y. From this fit transmittances smoothed in the y direction were calculated for six lateral distances, y = 0.5, 1.5, 4.5, 8.5, 13.5 and 39.5 μm. These distances were thought to be representative for the main features of the profiles at all Z and β. As an example of the extent of smoothing the original data and the fitted polynomial for a profile for Z = 20 and β = 0.5 is shown in Figure 2.

For each combination of Z and y a natural cubic spline function was fitted to the smoothed transmittance with β as the independent variable. From this function transmittances smoothed in the β direction were calculated for five velocities, β = 0.3, 0.4, 0.5, 0.6 and 0.7. In this way 30 condensed data points were obtained for each Z. The typical extent of smoothing is illustrated in Figure 3 which shows the transmittance and the corresponding cubic spline functions for Z = 20 at y = 0.5, 1.5, 4.5 and 13.5 μm as a function of β.

The overall effect of the smoothing for the particular profile shown in Figure 2 can be seen from the condensed data points for Z = 20 and β = 0.5 included in the Figure.

No smoothing was undertaken in the Z direction, although this would probably have eliminated the residual inconsistencies

in the data, some of which will be discussed in Section 5.3. The 150 condensed data points define the 25 profiles which have been used in the comparison with the theory in Section 5.

3. THEORY OF TRACK FORMATION

The basic assumption in Katz's theory is that the expected value $\langle n(t) \rangle$ of the volume grain density in the developed emulsion at a radial distance t from the track axis is

$$\langle n(t) \rangle = n_0 \left\{ 1 - \exp(- \bar{E}(t)/E_0) \right\}, \qquad (1)$$

where n_0 = the volume grain density in the undeveloped emulsion,

$\bar{E}(t)$ = the mean energy dose deposited by secondary electrons within a volume element V_0 at a radial distance t from the track axis, and

E_0 = the characteristic energy dose, i.e. the dose at which $\langle n \rangle = 0.63\ n_0$.

The numerical value of E_0 depends on the emulsion type and the processing conditions. The concept of exponential survival expressed by equation (1) follows from stochastic considerations (9). The qualitative validity of equation (1) has also been experimentally verified in, for instance, uniform electron exposure (14).

The mean energy dose $\bar{E}(t)$ is obtained from the point dose distribution E(t) for a homogeneous emulsion, i.e. an infinitely intimate mixture of gelatine and AgBr,

$$\bar{E}(t) = \frac{1}{V_0} \int_0^{r_0} E(t)\ 4\pi\ r^2\ dr, \qquad (2)$$

where $V_0 = \frac{4}{3}\ \pi r_0^3$ is the volume of a sphere with the same AgBr content as an average emulsion grain, the centre of the sphere

being located at t. Using the value of 0.27 μm for the diameter of an undeveloped grain in Ilford G5 emulsion, r_o turns out to be 0.17 μm.

In order to obtain the point dose distribution E(t) one needs to know the cross-section $d\sigma/d\omega$ for producing an electron with kinetic energy ω, the angular distribution of the emitted electrons, and their transport and energy dissipation in the emulsion. A discussion of these subjects has been delegated to the Appendix which also contains the derivation of the expression for the point dose distribution. This expression, given by equation (23) in the Appendix, is

$$E(t) = - \frac{N_e}{2\pi t} \int_I^{\omega_{max}} f(t,w) \frac{d\sigma}{d\omega} d\omega \ , \qquad (3)$$

where N_e = the volume density of electrons in the emulsion,

I = the mean excitation potential for the emulsion,

$\omega_{max} = 2 mc^2 \beta^2 / (1 - \beta^2)$ is the maximum energy transferable to an electron of mass m, and

$f(t,w)$ = the energy dissipated per unit length at a radial distance t by an electron of initial kinetic energy $w = \omega - I$.

The function f(t,w) has been calculated from the formula given by Kobetich and Katz (7). For the cross-section $d\sigma/d\omega$ we have used the second order Born approximation discussed in the Appendix. The distribution of Θ, the emission angle of the electrons, has been approximated by a δ-function at $\Theta = \frac{\pi}{2}$. Arguments for this choice can be found in the Appendix.

4. THEORETICAL TRANSMITTANCE PROFILES

4.1. Transmittance in parallel light

Let us consider a parallel beam of light incident parallel

to the z-axis at a lateral distance y from the axis of a track. In going through the distance dz the reduction of the radiant intensity I(y,z) will be

$$- dI(y,z) = I(y,z)\, \sigma_s\, \bar{n}(t)\, dz\ , \qquad (4)$$

where σ_s is the effective cross-section for removal of light from the parallel beam and $\bar{n}(t)$ is the volume density of the scattering centres responsible for this process. As the dip angles of the tracks are small, the radial distance t to the track axis is practically independent of x, i.e.

$$t^2 \simeq y^2 + z^2. \qquad (5)$$

If one assumes that the attenuation of the light beam is entirely due to the silver grains belonging to the track, one can put $\bar{n}(t) = \langle n(t) \rangle$, the quantity $\langle n(t) \rangle$ being defined by equation (1). Following Katz and Kobetich (8) we further assume that $\sigma_s = \alpha A$, A being the cross-sectional area of a developed grain and $\alpha < 1$ being a numerical factor which has to be determined from the experiment. In this formulation α should be interpreted as the multiplicative factor to the geometrical cross-section A which takes into account light scattering in the forward direction. Inserting these values into equation (4) and integrating between the limits z_1 and z_2 yields the transmittance, $\tau_p(y)$, in the parallel beam between these levels, where

$$\tau_p(y) = \frac{I(y,z_2)}{I(y,z_1)} = \exp\left\{ - \alpha\, A\, n_0 \int_{z_1}^{z_2} \left[1 - e^{-\bar{E}(t)/E_0} \right] dz \right\} \qquad (6)$$

The limits z_1 and z_2 should be chosen such that $\bar{E}(t) \ll E_0$ at each one of them. It must further be assumed that the beam is so narrow in the y direction that $\langle n(t) \rangle$ can be regarded as independent of y for all z in the interval $z_1 \leq z \leq z_2$.

4.2. Correction for a beam with large angular extension

For a parallel beam rescattering of light into the cone of acceptance is a second order effect, i.e. the transmittance above a solid layer of grains is expected to remain practically zero at all distances. In contrast to this, for the present photometer with its high numerical aperture rescattering is expected to have considerable importance. A theoretical treatment of the problem requires detailed knowledge of the scattering cross-sections and of the angular distribution of the radiant intensity within the cone of acceptance. Thus a theoretical treatment seems to be prohibitively difficult to carry out. For that reason we have, in the present investigation, made use of a semi-empirical model which has been proposed by Mathiesen in an initial study (15) of Katz's model. The basic idea is that the rescattered light flux at a given lateral distance, y, must depend on the number of scattering centres within the cone of acceptance and in its neighbourhood. This number in turn must be directly related to the absorptance within the regarded volume. If the correction is not too large and the variation of absorptance with lateral distance not too rapid, the absorptance within the regarded volume can be approximated with the absorptance $1 - \tau_p$ of the parallel beam at distance y. As the functional dependence between the rescattered light and the number of scattering centres is unknown, it seems appropriate to take a power series expansion of $1 - \tau_p$ as an approximation to $1 - \tau$, where τ is the actual transmittance at the lateral distance y. Thus,

$$1 - \tau = \sum_{\nu=0}^{N} a_\nu \, (1 - \tau_p)^\nu \, . \qquad (7)$$

The number of terms needed in this equation and the physical

interpretation of the constants a_ν will be discussed in Section 5.

4.3. Determination of adjustable parameters

Katz's theory contains two free parameters, E_o in equation (1) and α in equation (6). Of these E_o can in principle be determined from an independent measurement whereas α, which depends on the combined response of the photometer and the emulsion, must in general be determined from a fit to experimental profiles. In the preceding section we have introduced additional free parameters through the constants a_ν in equation (7). Before we can compare our experimental profiles with those calculated from the theory, we thus have to assign numerical values to all the free parameters. This has been done by fitting the theoretical profiles to the experimental data by means of a non-linear parameter optimization procedure. The quantity minimized by the procedure is the sum of the squares of the differences between calculated and experimental data which in the following is quoted as the 'square-sum'.

The experimental data used in the optimization procedure are strongly correlated. In the first place, the existence of small-scale differences in the photometer response in different parts of an emulsion sheet has been demonstrated in several investigations, including the stack used in the present study (16). In the second place, the procedure of data reduction and smoothing presented in Section 2.5 introduces additional strong correlation of the data. Therefore the total correlation coefficient is extremely difficult to calculate. For that reason we restrict ourselves to quote the square-sum as a crude measure of the goodness of fit. In comparing the square-sums obtained in different fits it should be kept in mind that the number of degrees of freedom depends on the number of parameters which are optimized

by the procedure. If not otherwise stated, all 150 condensed data points have been used in the different fits to be discussed in the next section.

5. RESULT AND DISCUSSION

5.1. The parameters E_o and α

The parameters E_o and α enter in all our calculations independently of different assumptions about a_v. We have found that although the values of E_o and α may vary by as much as 50 %, depending on the specific model used for the fit, the ratio α/E_o remains constant within a few per cent. This means that the optimization procedure is mainly sensitive to the ratio α/E_o and not to α and E_o separately. This is due to the way in which α and E_o appear in equation (6). Sensitivity to α/E_o at low values of $\bar{E}$ will become evident by expanding the inner exponential in equation (6), which for $E(t) \ll E_o$ becomes

$$\tau_p(y) \approx \exp\left[- A\, n_o \frac{\alpha}{E_o} \int_{z_1}^{z_2} \bar{E}(t)\, dz \right]. \qquad (7)$$

From equation (6) it is also evident that the numerical value of α depends on the values used for the volume grain density n_o and the projected area A of a developed grain. The average diameter of developed grains was estimated to be about 0.6 μm. The grain density n_o was calculated from the known density of AgBr and its partial density in the emulsion. Assuming that all AgBr crystals are uniform spheres with a diameter of 0.27 μm gave a value for $n_o = 47\ \mu m^{-3}$. The product $n_o A$ has been taken as $15\ \mu m^{-1}$.

Since α and E_o are algebraically interdependent, we have also made an independent determination of E_o. The method, which

has been proposed by Katz and Kobetich (8), was in this case based on a measurement of the plateau value of the linear grain density of singly charged particles. The linear grain density in tracks of weakly ionizing particles is, according to equation (1), given by

$$n = 2\pi n_0 \int_0^{t'} t \left[1 - e^{-\bar{E}(t)/E_0} \right] dt = \frac{2\pi n_0}{E_0} \int_0^{t'} t\, \bar{E}(t)\, dt, \quad (9)$$

where t', the upper limit of integration, should be taken as the radius of a cylinder within which the centre of a grain has to be located in order to be counted by the observer. Following Katz and Kobetich (8) we have used t' = 0.18 μm. This value together with the observed linear grain density, $n = 250\ \text{mm}^{-1}$, yields $E_0 = 10.5\ \text{keV}\ \mu\text{m}^{-3}$. Using this value of E_0 and a simplified form of equation (7),

$$1 - \tau = 1 - \tau_p + a_2 (1 - \tau_p)^2 . \quad (10)$$

yields $\alpha = 0.086$

and $a_2 = -0.22$ with the square-sum being 0.115. Using the same approximation but treating E_0 as an adjustable parameter the results were found to be $E_0 = 6.8\ \text{keV}\ \mu\text{m}^{-3}$, $\alpha = 0.057$ and $a_2 = -0.22$, with the square-sum being 0.116. The minimal change of the square-sum shows that no serious loss of generality can result if E_0 and α are kept constant at the values $E_0 = 10.5\ \text{keV}\ \mu\text{m}^{-3}$ and $\alpha = 0.086$. Unless otherwise stated, these values have been used in the following calculations.

5.2. The terms in the expansion of 1 - τ

In this section we discuss our model for taking into account the scattering of light as proposed in Section 4.2. First we discuss the three lowest order terms in equation (7) and make an attempt to give a physical interpretation of each of them. To

be able to do this different approximations to equation (7) have been made. These are listed in Table II together with the values obtained for the adjustable parameters when the theoretical profiles calculated for a given approximation are fitted to experimental data. At the end of the section the number of terms which should be included in equation (7) is discussed.

5.2.1 The constant term a_0. It is tempting to interprete the term a_0 as the absorptance due to background grains in the emulsion. As explained in Section 2.4, for an assumed parallel beam of light our normalization procedure should eliminate any contribution from the background. For a light cone with a large opening angle this need not necessarily be the case. If a_0 is assumed to be a background absorptance, the volume density n_b of background grains not properly taken into account by the normalization procedure can be estimated from

$$1 - a_0 = \exp\left[- \alpha A n_b (z_2 - z_1)\right] . \qquad (11)$$

Reasonable values of the constants yield a value of n_b in the range of 0.001 to 0.01 μm^{-3}, a figure which seems to be quite plausible.

In view of the speculative nature of the above interpretation we have also tried to find other explanations why the value of a_0 differs from zero. One possible reason could be an inability of our normalization procedure to fix the transmittance far from the track axis at the intended level of unity. In this respect random variations between different profiles certainly exist but we find it very difficult to explain a systematic error amounting to several per cent of the transmittance.

At any rate, for all approximations shown in Table II the magnitude of a_0 is seen to be so small that the contribution

from the constant term can be almost entirely ignored.

5.2.2 The linear term $a_1(1 - \tau_p)$. If equation (7) is approximated by the linear term only, the fit yields a value of $a_1 = 0.83$ as shown by approximation (a) in Table II. If scattering effects were negligible, i.e. $\tau = \tau_p$, the expected value clearly would be $a_1 = 1$. This seems to indicate that scattering of light is not properly taken into account by the parameter α alone and thus justifies the inclusion of the correction for rescattering discussed in Section 4.2.

However, it remains to be shown that manipulations on E_o or α cannot bring the theoretical profiles into accordance with experimental data under the assumption that $\tau = \tau_p$. This is exemplified in Figure 4 which shows the experimental profile for $Z = 26$ and $\beta = 0.3$, and corresponding theoretical profiles calculated for a range of values of E_o, keeping α fixed at $\alpha = 0.086$. According to Section 5.1 only minor changes in the quality of the fit can occur if α/E_o is kept constant. Thus it has not been necessary to repeat the calculations with different values of α. An inspection of Figure 4 shows that it is impossible to find a value of E_o which yields a reasonable agreement between observed and calculated profiles if it is assumed that $\tau = \tau_p$. We draw the conclusion that scattered light must be taken into account in addition to the dependence introduced by the parameter α.

The measured absorptance, averaged over the whole profile, is about 17 % smaller than the expected absorptance for a parallel beam of light. It seems plausible to assume that the magnitude of a_1 mainly reflects the number of scattering centres above the track, and although this idea has not been further pursued, we tentatively assume that a_1 in the first place is a function of the depth coordinate at which the measurement has been carried

out. In light of the track width measurements made in the present stack by Behrnetz et al. (16) this assumption seems to be very reasonable. The reduction in the mean track width level due to scattering of light observed by these authors between the air surface of the emulsion and the depth corresponding to the mean depth at which our profiles were taken is about 20 % in qualitative agreement with the value of $1 - a_1$ observed by us.

In the above approximation the constant term a_0 has been neglected. Including this term one obtaines the expansion of $1 - \tau$ to first power in $1 - \tau_p$, defined in Table II as approximation (c). As can be seen from Table II, the conclusions of the preceding paragraph remain valid also in this approximation.

5.2.3 The quadratic term $a_2 (1 - \tau_p)^2$. In a previous paper by Mathiesen (15) where the general idea of the expansion according to equation (7) was proposed, the particular approximative form given by equation (10) was shown to yield a good description of experimental profiles. For that reason the approximation has been included also in the present study. The results are shown on line (b) in Table II. As can be seen by the square-sums quoted for approximations (a) and (b) in Table II, the use of a quadratic term together with the linear term with $a_1 = 1$ constitutes a substantial improvement over the approximation based on the linear term $a_1 (1 - \tau_p)$ only. Note that the number of degrees of freedom is the same in the two cases. The improvement is most pronounced at the flanks of the profiles where the effects of a high numerical aperture should be easiest to see. Therefore we tentatively assume that the magnitude of the constant a_2 is related to the numerical aperture of the instrument. Although we cannot prove this assumption on the basis of the

present study, the results to be presented in a forthcoming paper (17) seem to confirm the idea.

If the expansion of $1 - r$ according to equation (7) is carried out to second power in $1 - \tau_p$ one obtains the approximation studied as case (d) in Table II. As can be seen from a comparison with approximation (b) in Table II the result of the fit is almost the same in both cases. This supports the relevance of the approach in the initial study (15) and indicates that our interpretation of the constants a_0, a_1 and a_2 seems to be valid also when they are used simultaneously.

5.2.4 Higher order terms. We have no a priori knowledge of the number of terms needed in equation (7). In choosing the approximate number we should be guided by the goodness of fit as expressed by the square-sum. The results using an expansion to third power in $1 - \tau_p$ are shown as approximation (e) in Table II. As can be seen from a comparison of the expansions to second and third power in $1 - \tau_p$, the inclusion of the fourth term does not improve the fit noticeably. The tendency of the square-sum to become independent of the number of terms has been further proved by using an expansion to fifth power in $1 - \tau_p$. In this case the square-sum was found to be 0.089, i.e. a reduction of only 3 % over the value found for the expansion to third power in $1 - \tau_p$. On account of this we have chosen to use an expansion to the second power in $1 - \tau_p$. It should be pointed out that the asymptotic value of the square-sum mainly reflects the internal inconsistency of our experimental data.

As can be seen from Table II, the results obtained for the complete expansion to second power, given by approximation (d), and the simplified form, given by approximation (b), are nearly identical. Because the total number of adjustable parameters

should be kept as low as possible, we propose to use the full expansion to second power in $1 - \tau_p$ if E_o and a are known from other sources, and the appxorimation given by equation (10) if E_o and a have to be determined from the fit.

5.3. Comarison between observed and calculated profiles

In Figure 5 we show our condensed data points for Z = 14, 16, 20, 24, 26 and β = 0.3, 0.4, 0.5, 0.6, 0.7 together with the corresponding profiles calculated from the theory, using for $1-\tau$ an expansion to second power in $1-\tau_p$. The numerical values of the constants in this expansion were those of case (d) in Table II.

The general agreement between theory and experiment in Figure 5 is seen to be surprisingly good, considering the low number of adjustable parameters. The only appreciable systematic difference occurs at the profile for Z = 24 and β = 0.3. This is most probably due to the low number of tracks for Z = 24, and in particular the total absence of experimental data for β = 0.4. As a result of this the smoothing procedure in the β direction has failed at the lower range of the β interval. If the erroneous profile were replaced by absorptances obtained by linear interpolation between corresponding values for Z = 20 and Z = 26, all the interpolated values would touch the theoretical profile if represented by circles of the same size as those used for the original data points in Figure 5.

The encourageing agreement between theory and experiment shown in Figure 5 was obtained using four free parameters for the theoretical profiles. It should be pointed out that the agreement would have been almost equally good if the theoretical profiles instead were based on equation (10), i.e. on a model which contains only two adjustable parameters.

5.4. Extrapolation of profiles outside the range of Z and β

The crucial test of the usefulness of the theory is to see how well it can predict transmittance profiles outside the range of Z and β used for the determination of the free parameters.

A series of such tests has been carried out, using only a limited number of the experimental profiles for the fit. In keeping with the recommendation made at the end of Section 5.2 E_0 and α were treated as free parameters and $1 - \tau$ was approximated by equation (10). In Table III the particular combinations of transmittance profiles used in the fit and the resulting values of E_0, α and a_2 are listed. Also included in Table III is the ratio α/E_0. By the argument given in Section 5.1 constancy of this ratio implies that the quality of the fit can be expected to remain unchanged if the variations in E_0 or α are not extensive. An inspection of Table III shows that in all tests α/E_0 as well as a_2 deviate very little from the values shown on the first line, i.e. for a fit based on all experimental profiles. The square-sum for this fit, (b) in Table II, demonstrates that in this case the calculated profiles agree well with experimental data. Thus there is indirect evidence that in all the tests shown in Table III there is a reasonable agreement between predicted and experimental profiles. For some of the tests we have verified this explicitly by direct comparison of predicted profiles with experimental data. Examples of such a comparison for the test shown on the second line in Table III have been given in our preliminary report (10).

Our conclusion is that within the range of Z and β investigated in the present study the track formation theory is capable of predicting the transmittance profiles with reasonable accuracy from rather scanty experimental data, with regard to either the number of different β or Z values included in the fit.

The very promising result of the present study has encouraged us to pursue the further applicability of the theory of track formation in its present form. In a forthcoming paper [19] we will compare theoretical predictions with track width measurements both in the present and in a different stack of emulsions, and with profile measurements by another type of photometer in a different emulsion stack.

APPENDIX

THE POINT DOSE DISTRIBUTION

As mentioned in Section 3 the calculation of the point dose distribution must be based on a knowledge of (a) the cross-section $d\sigma/d\omega$ for producing an electron with kinetic energy in the interval $(\omega, \omega+d\omega)$, (b) the angular distribution of the emitted electrons, and (c) the transport of electrons and their energy dissipation. In this Appendix these subjects will be discussed in some detail and the derivation of an expression for the point dose distribution E(t) will be outlined.

A.1 The cross-section for electron production

Close collisions. For the formation of tracks investigated in the present study the most important contribution to $d\sigma/d\omega$ comes from close collisions, i.e. such encounters where the amount of energy transferred to the electron is much larger than the binding energy of the electron. This cross-section can be obtained from the exact Mott phase-shift formula for elastic electron scattering from a stationary point-charge nucleus (see e.g. Motz et al. (18)).

The cross-sections $d\sigma/d\Omega'$ quoted in reference (17) yield the probability of scattering of an electron with velocity βc (Lorentz

factor $\gamma=(1-\beta^2)^{-1/2}$) into an element $d\Omega'$ of the solid angle around the scattering angle θ', i.e.

$$d\Omega' = 2\pi \sin\theta' \, d\theta' \tag{12}$$

The kinetic energy ω of the electron in the frame of reference where the electron is initially at rest is obtained by a Lorentz transformation,

$$\omega = \omega_{max} \sin^2 \frac{\theta'}{2} \quad , \tag{13}$$

where

$$\omega_{max} = 2 mc^2 \beta^2 \gamma^2 \tag{14}$$

is the maximum energy transferrable to an electron of mass m, assumed to be much lighter than the scatterer. From equations (12) and (13) it is readily seen that

$$\frac{d\sigma}{d\omega} = \frac{4\pi}{\omega_{max}} \frac{d\sigma}{d\Omega'} \quad . \tag{15}$$

From the Lorentz transformation one also obtains the following relationship between θ' and the emission angle θ of the scattered electron with respect to the velocity vector of the impinging ion,

$$\gamma \tan\theta \tan \frac{\theta'}{2} = 1 \ . \tag{16}$$

From equations (13), (14) and (16) it is seen that

$$\cos^2\theta = \frac{\omega}{\omega_{max}} \frac{\omega_{max} + 2 mc^2}{\omega + 2 mc^2} \tag{17}$$

Unfortunately the exact Mott cross-section $(d\sigma/d\omega)_M$ cannot be given in a closed form. Evaluation of $(d\sigma/d\omega)_M$ is possible by numerical methods (19,20) but the computation is complicated. The closest approximation to $(d\sigma/d\omega)_M$ which still can be given in a reasonably comprehensive form is known as the third Born approximation (Formula 1A-106 of reference (18)),

$$\left(\frac{d\sigma}{d\omega}\right)_3 = \left(\frac{d\sigma}{d\omega}\right)_0 \left\{1 - \beta^2\zeta^2 + \pi\alpha Z\beta\zeta \quad (1-\zeta) + \right.$$

$$+ \alpha^2 Z^2 \left[(\zeta + \beta^2\zeta^2)L_2(1-\zeta^2) - 4\zeta L_2(1-\zeta) + \zeta^2 \ln^2\zeta (2+\beta^2\zeta^2/(1-\zeta^2)) + \right.$$

$$\left. \left. + \frac{\pi^2}{12}(6\zeta - 4\zeta^2 + \beta^2\zeta^2(1-5\zeta)/(1+\zeta))\right]\right\}. \qquad (18)$$

In this equation

$\zeta^2 = \omega/\omega_{max}$,

$\alpha = e^2/(2\varepsilon_0 hc)$ is the fine structure constant in SI units,

$L_2(y) = \int_0^y \frac{1}{x} \ln(1-x)dx$ is Eulers dilogarithm, and

$\left(\frac{d\sigma}{d\omega}\right)_0 = \frac{2\pi r_0^2 \, mc^2 Z_e^2}{\beta^2 \, \omega^2}$ is the Rutherford cross-section, where

$r_0 = e^2/(4\pi\varepsilon_0 \, mc^2)$ is the classical electron radius in SI units

and

$Z_e = Z\left[1-\exp(-130\,\beta Z^{-2/3})\right]$ is the effective charge number

as given by Pierce and Blann (21).

The first and second Born approximations, $(d\sigma/d\omega)_1$ and $(d\sigma/d\omega)_2$, are obtained if two and three terms respectively are kept in the braces of equation (18). It seems worthwhile to recall the statement made by McKinley and Feshbach (22) that the expression for $(d\sigma/d\Omega')_2$ originally given by Mott (23) is in error. This statement implies that the corresponding expression for $(d\sigma/d\omega)_2$ which was obtained by Bradt and Peters (24) and since then has been extensively used by cosmic ray physicists, also is in error.

Using the data for the exact Mott cross-section $(d\sigma/d\omega)_M$ calculated by Doggett and Spencer (19), we have investigated the departure of $(d\sigma/d\omega)_i$ (i = 0,1,2,3) from the exact Mott cross-section for the range of Z and β which is of interest in the present work. The results are shown in Figure 6. We wish to emphasize that the limiting condition of validity of the

different cross-section formulae, $\alpha Z_e/\beta \gg 1$ for $(d\sigma/d\omega)_0$ and $(\alpha Z_e/\beta)^i \ll 1$ for $(d\sigma/d\omega)_i$ $(i=1,2,3)$, is not fulfilled for all cases shown in Figure 6.

When comparing the relative accuracy of the different approximations shown in Figure 6 it should be borne in mind that ω_{max} is a function of the particle velocity through equation (14) and that the number of electrons with energy ω is according to equation (18) approximately proportional to ω^{-2}. This means that the main contribution to the energy dissipated at a given distance from the path of the ion is due to electrons with quite different values of ω/ω_{max}, at different particle velocities. For instance, if one is only interested in the energy dissipated by δ-rays with $\omega < 100$ keV, it can be seen that in the range of β and Z displayed in Figure 6 the Rutherford cross-section is even a better approximation than the first Born cross-section, especially at low velocities. This may justify the approximation $d\sigma/d\omega \approx (d\sigma/d\omega)_0$ made in Katz's original theory (8).

In our calculations we have chosen to approximate $d\sigma/d\omega$ by $(d\sigma/d\omega)_2$ due to the lesser complexity of this cross-section formula compared with higher order Born approximations, in spite of the fact that even the condition of validity of the second Born approximation is poorly met at our lowest values of β and highest values of Z. As can be seen from Figure 6 the error committed in doing this must be negligible in comparison with other sources of error.

Distant collisions. The contribution to $d\sigma/d\omega$ from distant collisions cannot be easily evaluated. Clearly, if the energy imparted to an atomic electron is comparable to or smaller than the binding energy of the electron, the Mott cross-section cannot be used. In this region $d\sigma/d\omega$ becomes a function of the atomic

properties of the absorbing medium and the evaluation of the cross-section must be based on the knowledge of the oscillator strengths of all the atoms involved. The relevant theory can be found in the excellent review paper by Inokuti (25). Some guidance about $d\sigma/d\omega$ for distant collisions might also be obtained from the theory of binary encounters. A current formulation of this theory can be found in the paper by Rudd et al. (26). Using more approximative methods Fowler et al. (27) have estimated the contribution from distant collisions to the energy deposition in nuclear emulsion. According to these authors the contribution is approximately 10 % of the total. Included in this figure is the contribution from the electromagnetic de-excitation of the atoms of the absorbing medium. Furthermore, the radial dependence of the energy deposition from these sources is found to be very nearly the same as the radial dependence obtained for energy deposition from close collisions. By this argument, neglecting the contribution to $d\sigma/d\omega$ from distant collisions cannot introduce any large error in our calculation of $\langle n(t) \rangle$, because a moderate t-independent scaling of $\bar{E}(t)$ can easily be compensated for by a proper choice of E_0. Consequently the contribution to $d\sigma/d\omega$ from distant collisions has not been taken explicitly into consideration in our calculations.

A.2 The angular distribution of the emitted electrons

For close collisions the emission angle θ of an electron with energy ω, originating in an encounter with an ion with velocity βc is uniquely determined from equations (14) and (17). It can be mentioned that in the literature dealing with relativistic ions the non-relativistic approximation

$$\cos \theta = \frac{\omega}{\omega_{max}} \qquad (19)$$

to equation (17) often is used in spite of its being correct only at the limit $\beta^2\gamma^2 \ll 1$.

In Figure 7 we compare the differential cross-sections $(d\sigma/d\Omega)_2$ obtained from equation (18) in the second Born approximation, assuming that the functional dependence of ω on θ is given by equations (17) and (19) respectively. The solid angle element $d\Omega$ is defined by

$$d\Omega = 2\pi \sin\theta \, d\theta. \qquad (20)$$

The calculations are made for Z=26, but, however, within the scale of Figure 7 the difference for other charge numbers of interest in the present study is barely distinguishable. It can be mentioned that the scale of the ordinate in Figure 7, with good approximation, also can be interpreted as the number of δ-rays per cm and steradian for Z=1 in nuclear emulsion. For orientation purposes a number of electron energies ω calculated from equations (17) and (19) are shown in the diagram. As seen from Figure 7 the cross-section is underestimated if the functional dependence between ω and θ is taken from equation (19). At $\theta=0$ and $\theta=\frac{\pi}{2}$ the cross-section is found to be smaller by a factor $1-\beta^2$. The error is larger at intermediate values of θ and the maximal error which is approximately $(1-\beta^2)^2/(1-\frac{1}{2}\beta^2)^2$ occurs at $\cos^2\theta \approx (2-\beta^2)^{-1}$.

When using the angular distribution obtained from either equation (17) or equation (19) two points should be borne in mind. The first one concerns the theoretical range of validity of these equations. Because they are derived for close collisions, the angular distribution obtained from them can be expected to be correct only as long as the energy imparted to the electron is well above the binding energy of the electron in an atomic shell. As seen from Figure 7 this can be a rather

serious limitation. When the close collision approximation fails, the calculation of the angular distribution becomes extremely difficult for all but hydrogen targets, cf. Rudd et al. (28).

The second point concerns the practical value of a knowledge of the angle θ. Due to the extensive scattering of electrons this angle defines the direction of the electron's path correctly only at the very instant of emission. Because the scattering is more pronounced at low electron energies, the uncertainty about the true direction of the electron's path can be expected to increase with decreasing initial electron energy. From the point of view of energy deposition around the ion's path, the effect of electron scattering is seen to be most harmful for electrons ejected at small angles relative to the ion trajectory. Thus it can be expected that a theoretical energy dose distribution based on a kinematically correct angular distribution, but utilizing electron energy dissipation data based on normally incident electrons' penetration of thin slabs of material, will come into greater and greater disagreement with experimental dose distributions, the lower the ion velocity is. This effect has been observed by Mathiesen in an earlier study (15). In this study it was found that a model based on the angular distribution derived from equation (17) was unable to predict the profiles of iron tracks at $\beta \leq 0.4$ whereas a much better fit was obtained if it was assumed that all electrons are ejected at right angles to the ion's path. In view of the result of this earlier work we have in the present study approximated the angular distribution with a δ-function at $\theta = \frac{\pi}{2}$.

A.3 The electron energy dissipation

The dissipation of electron energy around the path of the

heavy ion can in principle be obtained by solving the transport equation for a line source emitting monoenergetic electrons at a fixed angle to the line. However, as shown by Spencer (29), the solution of the transport equation is extremely complicated already for a plane perpendicular source, and to our knowledge no solution for a line source has been worked out. Therefore the electron energy dissipation is usually based on data obtained from the plane perpendicular geometry. For this geometry Kobetich and Katz (7) have devised an empirical formula according to which the energy dissipated per unit length at a distance t from the source is given by

$$f(t,w) = \frac{d}{dt}\left[\eta(t,w)\ W(t,w)\right] \quad , \tag{21}$$

where η = the probability that an electron of initial energy w will penetrate the thickness t, and

W = the residual energy at that distance.

Both η and W depend on the atomic number of the absorber with the functional dependence being determined from experimental data in the slab geometry. The differentiation with respect to t can be carried out analytically.

Within the limitations stated in reference (7), equation (21) should be reasonably accurate for electrons ejected normally to the ion's path. According th Section A.2 this simplifying assumption has been made in the present calculation. Consequently the electron energy dissipation has been estimated from equation (21).

It can be anticipated that equation (21) would become less accurate the smaller the ejection angle is. Therefore, when it is attempted to use a more realistic angular distribution than that of the present study, the electron energy dissipation should be calculated from a model which explicitly considers the

transport of electrons ejected at oblique angles to the ion's path. One very promising possibility would be to use the set of Monte Carlo calculations presented by Berger (30), especially if such calculations become available also for higher electron energies.

A.4 The point dose distribution

Combining the cross-section $d\sigma/d\omega$ with the probability η and the residual energy W defined in Section A.3, the energy ε transported through a cylinder whose axis coincides with the ion trajectory is seen to be

$$\varepsilon = \ell\, N_e \int_{\omega_o}^{\omega_{max}} \eta(t,w)\; W(t,w)\; \frac{d\sigma}{d\omega}\, d\omega\ , \qquad (22)$$

where t is the radius of the cylinder and ℓ its length, and N_e is the volume density of electrons in the absorber. The lower limit of the integration, ω_o, should be chosen at sufficiently high energy to justify the close collision approximation of $d\sigma/d\omega$. However, following the procedure adopted by Katz and Kobetich (8), we have put ω_o equal to the mean excitation potential for nuclear emulsion, I = 320 eV. The error committed in doing this seems to be negligible, because even a much higher value of ω_o would yield $\bar{E}(t) \gg E_o$ in the vicinity of the track axis for all β and Z in the present work, i.e. $\langle n(t)\rangle \approx \eta_o$ according to equation (1). The relation between ω and the initial kinetic energy w of the electron can according to Rudd et al (28) be approximated by $\omega = w + I$.

The point dose distribution E(t) is finally found by differentiating equation (22) with respect to t,

$$E(t) = -\frac{1}{2\pi\ell t}\frac{d\varepsilon}{dt} = -\frac{N_e}{2\pi t}\int_{I}^{\omega_{max}} f(t,w)\,\frac{d\sigma}{d\omega}\,d\omega. \qquad (23)$$

Table I

The number of tracks used at each β and Z

Z \ β	0.30	0.40	0.50	0.55	0.60	0.65	0.70	0.75	0.80
14	3	4	4	4	4	4	4	2	-
16	3	3	4	4	4	4	3	-	-
20	2	2	4	4	5	4	3	-	-
24	3	-	3	4	3	4	3	-	-
26	3	5	6	5	6	6	6	6	5

Table II

Approximations to equation (7)

Approximation of $1-\tau$ in terms of $1-\tau_p$	Values (assumed or) obtained in the fit				
	a_0	a_1	a_2	a_3	square-sum
(a) $a_1(1-\tau_p)$	(0)	0.83	-	-	0.195
(b) $1-\tau_p + a_2(1-\tau_p)^2$	(0)	(1)	-0.22	-	0.115
(c) $\sum_{\nu=0}^{1} a_\nu(1-\tau_p)^\nu$	0.03	0.78	-	-	0.129
(d) $\sum_{\nu=0}^{2} a_\nu(1-\tau_p)^\nu$	0.015	0.93	-0.16	-	0.105
(e) $\sum_{\nu=0}^{3} a_\nu(1-\tau_p)^\nu$	0.003	1.17	-0.84	0.48	0.092

Table III

Fitted values of E_o, α and a_2 based on a limited number of experimental profiles

Profiles used for the fit											Values of the fitted parameters			
Z					β						E_o	α	$-a_2$	α/E_o
14	16	20	24	26	0.3	0.4	0.5	0.6	0.7	0.8	keV μm^{-3}			μm^3 MeV^{-1}
x	x	x	x	x	x	x	x	x	x		6.83	0.0570	0.22	8.35
x	x	x	x	x			x	x	x		6.81	0.0571	0.22	8.38
x	x	x	x	x	x	x	x				4.94	0.0420	0.18	8.50
x	x	x	x	x	x		x				4.89	0.0415	0.18	8.49
				x		x	x	x	x	x	5.24	0.0429	0.20	8.19

Figure captions

Fig. 1. A schematic diagram of the photometer.

Fig. 2. Experimental data points (circles) and smoothed transmittance profile (curve) for Z = 20 and β = 0.5. Also shown are condensed data points (crosses) obtained after additional smoothing in the β direction.

Fig. 3. The effect of the smoothing of average transmittances along the β direction for Z = 20 at four different lateral distances y from the track axis.

Fig. 4. Experimental absorptance profile for Z = 26 and β = 0.3 (dashed curve) and corresponding theoretical profiles (full curves) calculated for a parallel beam of light for five different ratios of α/E_0.

Fig. 5. Comparison between experimental and theoretical absorptance profiles for the full range of Z and β values investigated in the present study. The theoretical profiles are calculated using approximation (d) in Table II.

Fig. 6. The ratio R_i of the i-th Born approximation cross-section $(d\sigma/d\omega)_i$ to the exact Mott cross-section $(d\sigma/d\omega)_M$ as a function of the electron energy ω in units of the maximum electron energy ω_{max}. The ratio R_i is found from $R_i = \eta - n/4$ where η is the ordinate and n is a displacement factor displayed in the Figure. i = 0 (Rutherford cross-section; dotted curve), i = 1,2,3 (first to third Born approximations; dashed, full, and dot-dashed curves). Calculations are for Z = 14 and 26 and β = 0.42, 0,6 and 0.8.

Fig. 7. The second order Born cross-section $(d\sigma/d\Omega)_2$, differential in the solid angle Ω of the emitted electrons, as a function of cosinus for the emission angle θ, for an assumed classical relationship between β and electron energy ω (equation (19), dashed curve) and the corresponding relativistically correct relationship (equation (17), full curve). Calculations are made for β = 0.2, 0.4, 0.6 and 0.8. The positions of ω = 1, 10, 100 and 1000 keV are indicated on the curves.

REFERENCES

1. H. Messel and D.M. Ritson,
Phil. Mag. 41. 1129 (1950).

2. M. Jensen, L. Larsson and R. Rosander,
Nucl. Instr. Methods 104, 611 (1972).

3. P.G. Bizzeti and M. Della Corte,
Nuovo Cimento 11, 317 (1959).

4. Robert Katz and J.J. Butts,
Phys. Rev. 137, B198 (1965).

5. E.J. Kobetich and Robert Katz,
Phys. Rev. 170, 391 (1968).

6. E.J. Kobetich and Robert Katz,
Phys. Rev. 170, 405 (1968).

7. E.J. Kobetich and R. Katz,
Nucl. Instr. Methods 71, 226 (1969).

8. Robert Katz and E.J. Kobetich,
Phys. Rev. 186, 344 (1969).

9. R. Katz, S.C. Sharma and M. Homayoonfar,
Nucl. Instr. Methods 100, 13 (1972).

10. M. Jensen, L. Larsson, O. Mathiesen and R. Rosander,
Conf. Papers, 13th Intern. Cosmic Ray Conf.,
Vol. 1, p 2942, Denver, U.S.A., 1973.

11. M. Jensen, L. Larsson, O. Mathiesen and R. Rosander,
Radioprotection 9, No. 1, 7 (1974).

12. L. Jacobsson, G. Jönsson, K. Söderström and H. Håkansson,
Nucl. Instr. Methods 112, 575 (1973).

13. K. Söderström, S. Lindstam, S. Behrnetz and K. Kristiansson,
Astrophys. Sp. Sci. 21, 211 (1973).

14. J.F. Hamilton,
Electron-Beam Exposures,
in The Theory of the Photographic Process,
Ed. C.E.K. Mees and T.H. James, 3rd. ed.,
The Macmillan Company, New York 1966.

15. O. Mathiesen,
Proc. 8th Intern. Conf. on Nuclear Photography and SSTD,
10-15 July 1972, Bucharest Roumania , Vol. 1, p 47.

16. S. Behrnetz, K. Kristiansson, S. Lindstam and K. Söderström,
Cosmic Ray Physics Report LUIP-CR-73-01, Lund, Sweden, 1973.

17. M. Jensen and O. Mathiesen,
to be published.

18. J.W. Motz, Haakon Olsen and H.W. Koch,
Rev. Mod. Phys. 36, 881 (1964).

19. J.A. Doggett and L.V. Spencer,
Phys. Rev. 103, 1597 (1956).

20. S.H. Morgan and P.B. Eby,
Nucl. Instr. Methods 106, 429 (1973).

21. T.E. Pierce and M. Blann,
Univ. of Rochester Report No. 3591-8,
Rochester, USA, 1968.

22. W.A. McKinley, Jr., and H. Feshbach,
Phys. Rev. 74, 1759 (1948).

23. N.F. Mott,
Proc. Roy. Soc. (London), A 124, 425 (1929).

24. H.L. Bradt and B. Peters,
Phys. Rev. 74, 1828 (1948).

25. Mitio Inokuti,
Rev. Mod. Phys. 43, 297 (1971).

26. M.E. Rudd, D. Gregoire and J.B. Crooks,
Phys. Rev. A 3, 1635 (1971).

27. P.H. Fowler, V.M. Clapham, V.G. Cowen, J.M. Kidd and
R.T. Moses,
Proc. Roy. Soc. (London) A 318, 1 (1970).

28. M.E. Rudd, C.A. Sautter and C.L. Bailey,
Phys. Rev. 151, 20 (1966).

29. L.V. Spencer,
National Bureau of Standards Monograph 1 (1959).

30. M.J. Berger,
Proc. Third Symposium on Microdosimetry, Stresa (Italy),
October 18-22, 1971, Ed. H.G. Ebert, EURATOM EUR 4810 d-f-e,
p 157.

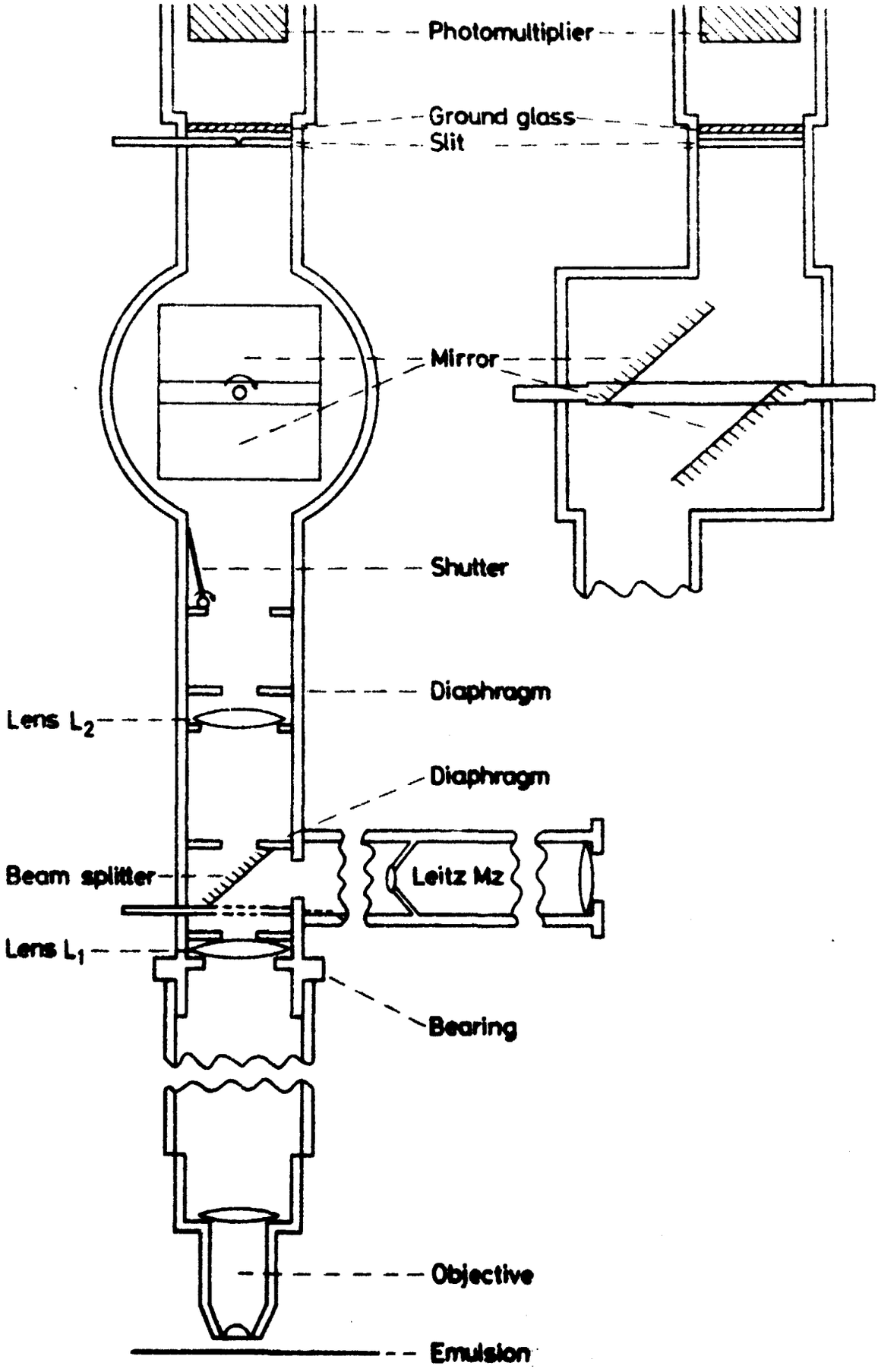
Photomultiplier
Ground glass
Slit
Mirror
Shutter
Diaphragm
Lens L_2
Diaphragm
Beam splitter
Leitz Mz
Lens L_1
Bearing
Objective
Emulsion

Fig. 1

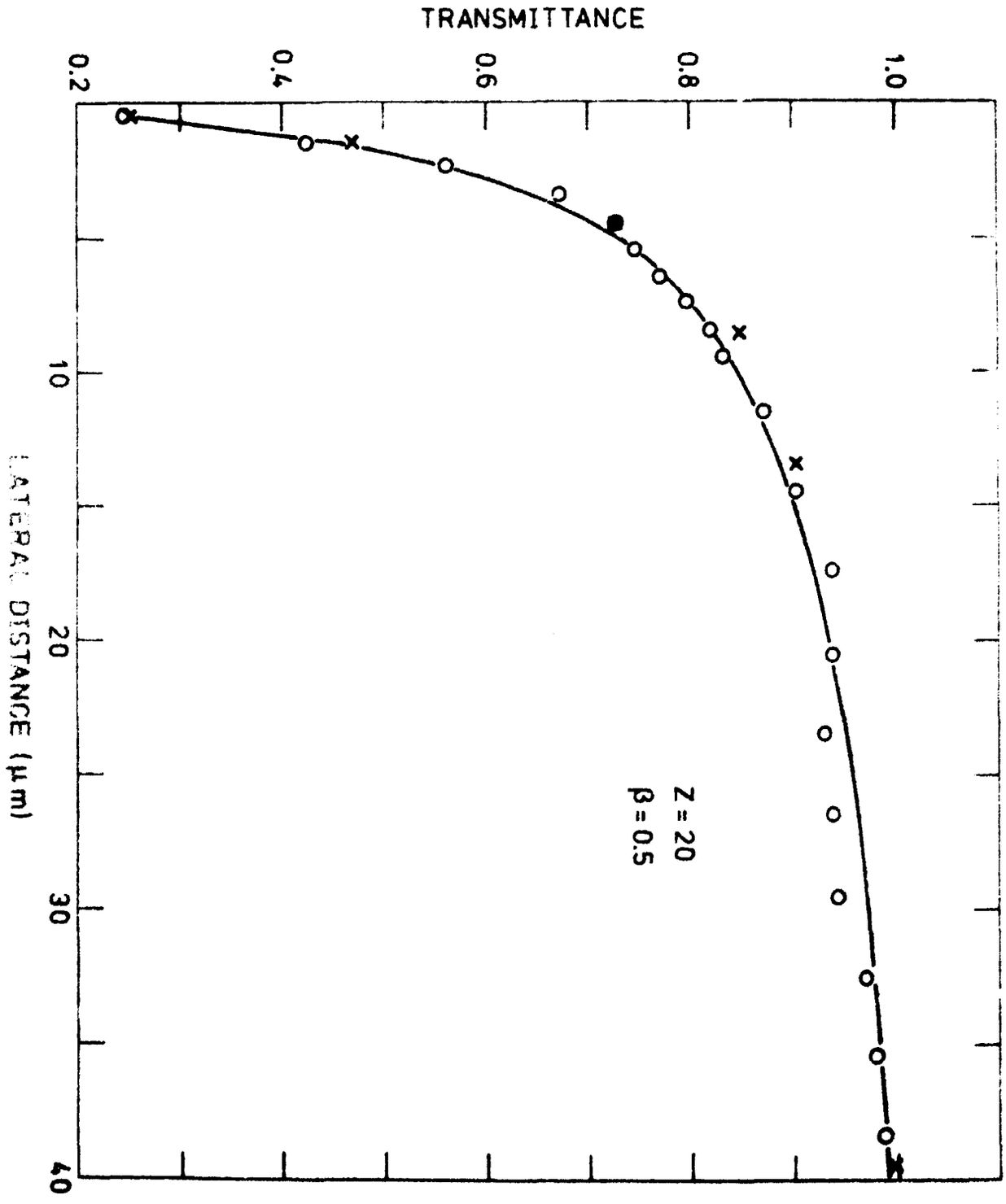
TRANSMITTANCE
0.2
0.4
0.6
0.8
1.0
10
20
30
40
LATERAL DISTANCE (μm)
Z = 20
β = 0.5

Fig. 2

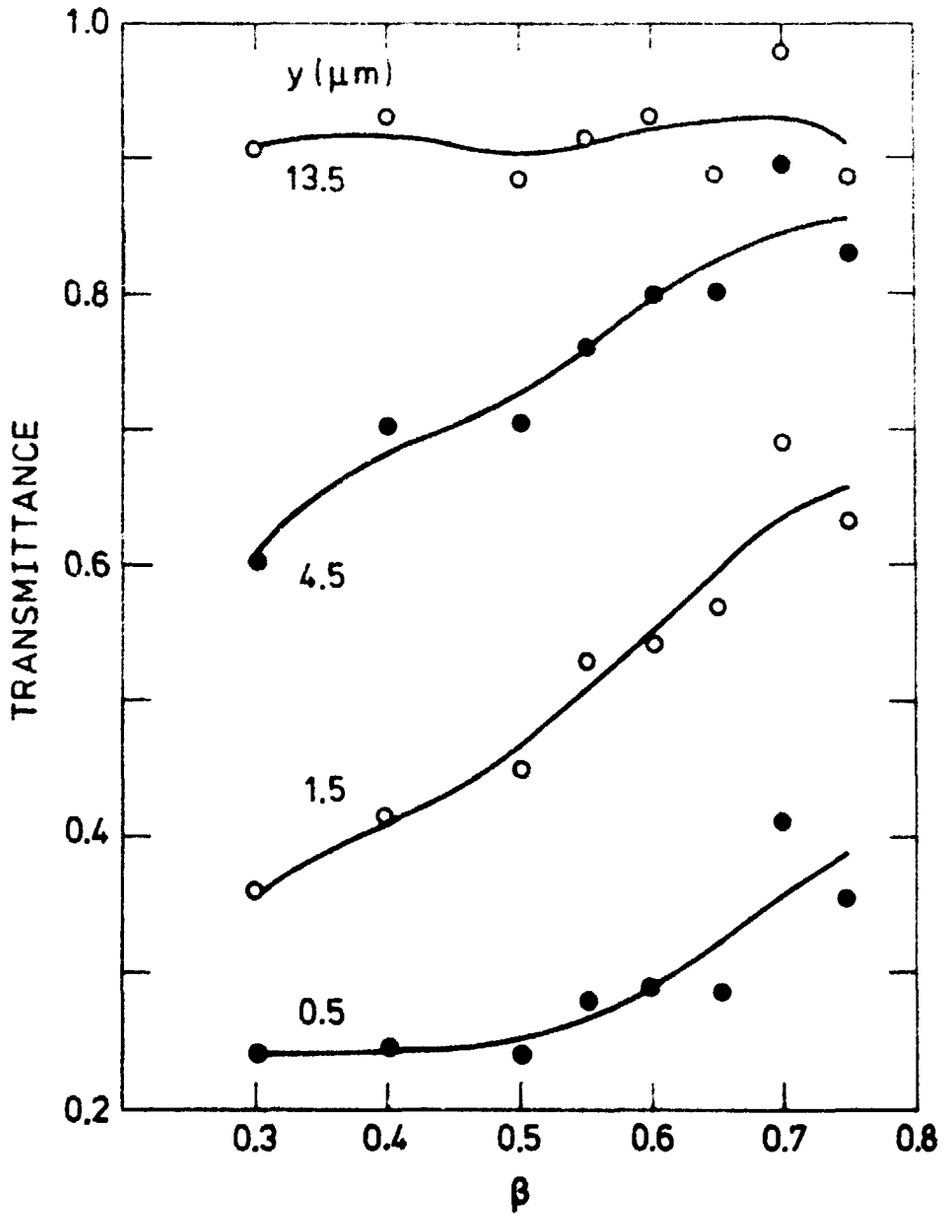

Fig.3

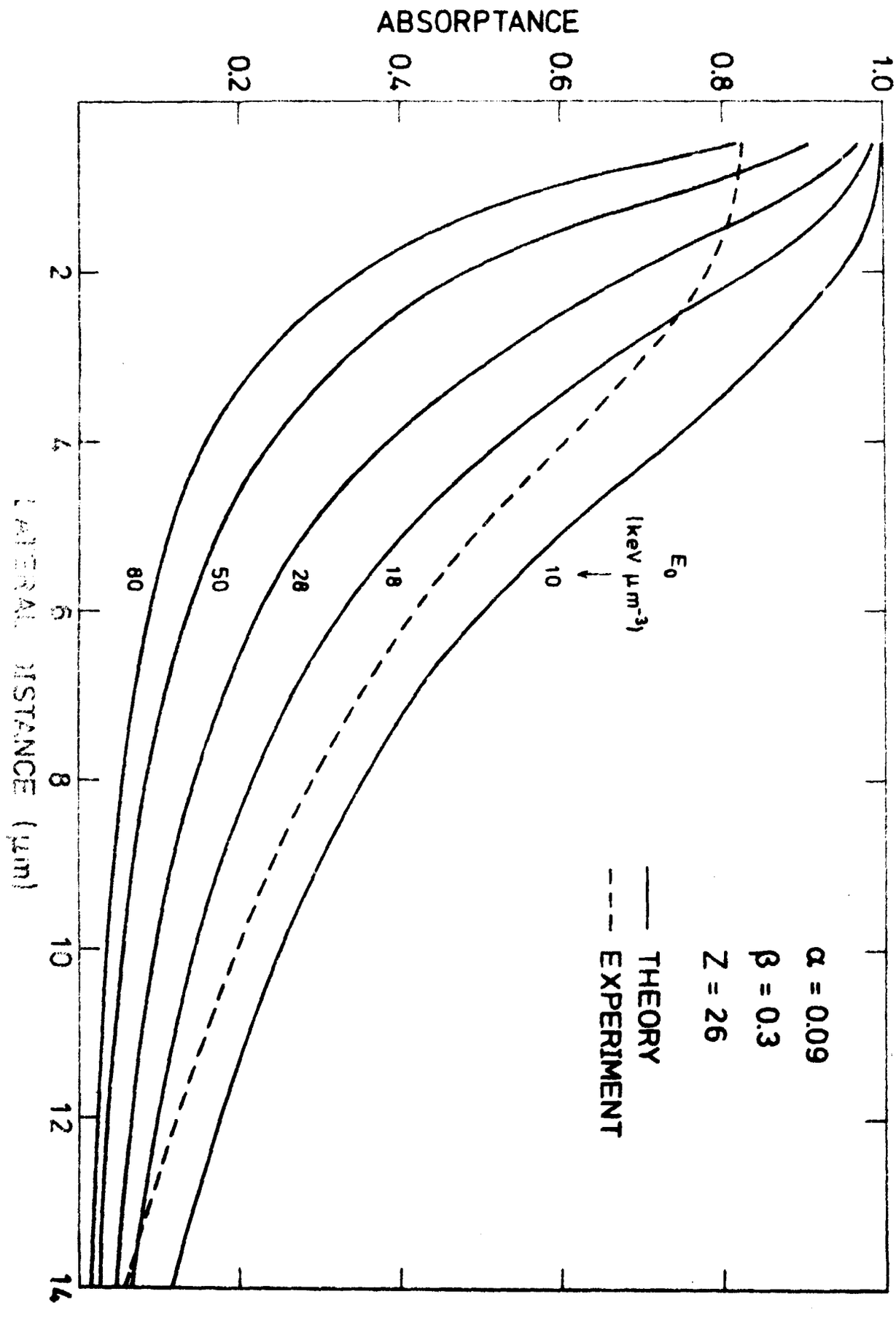
ABSORPTANCE
0.2
0.4
0.6
0.8
1.0
2
4
6
8
10
12
14
(μm) DISTANCE INTERNAL
80
50
28
18
10
E_0
(keV μm^{-3})
α = 0.09
β = 0.3
Z = 26
THEORY
EXPERIMENT

Fig.1

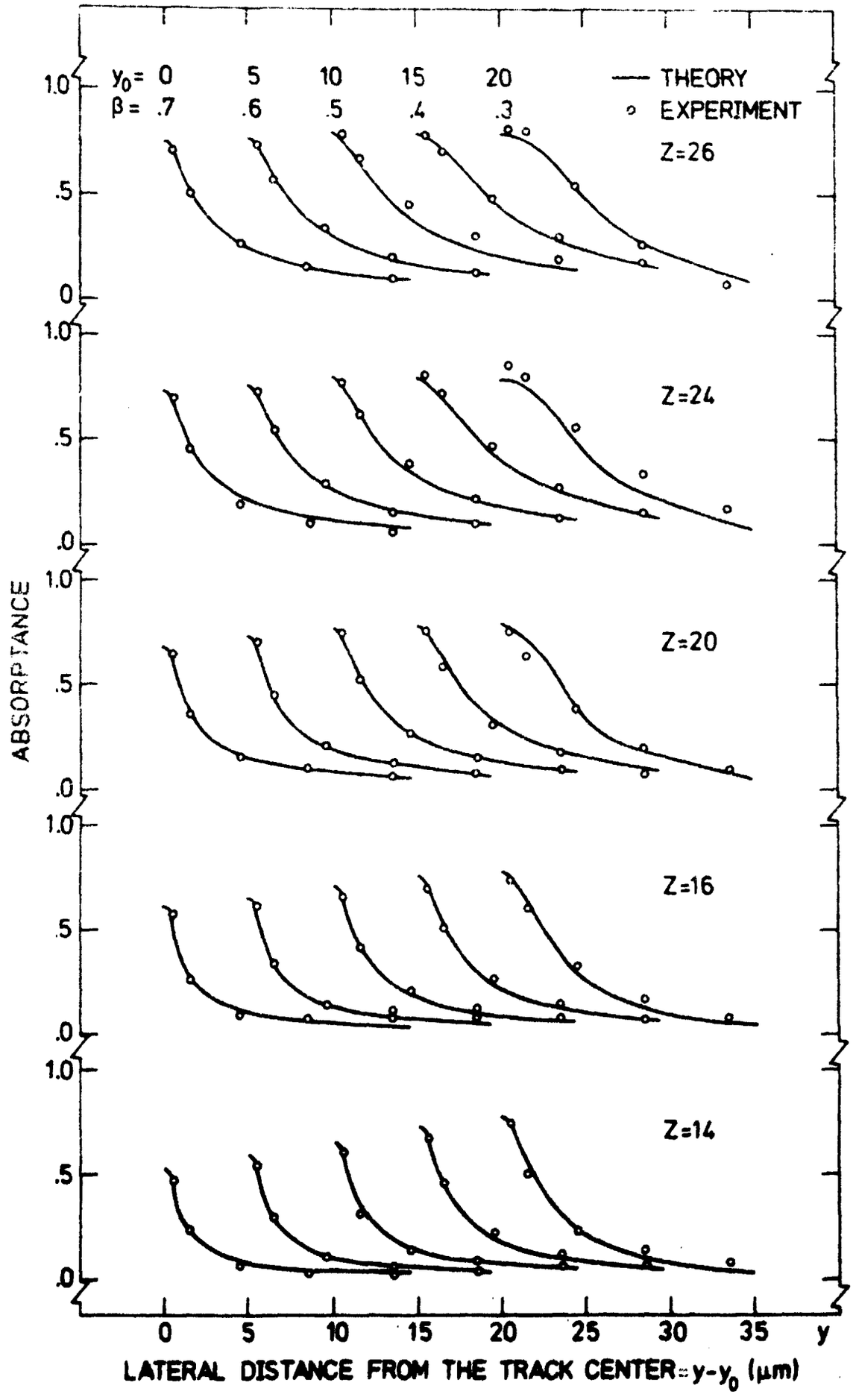
y_0= 0 5 10 15 20
β = .7 .6 .5 .4 .3
THEORY
EXPERIMENT
Z=26
Z=24
Z=20
Z=16
Z=14
ABSORPTANCE
1.0
.5
0
.0
0 5 10 15 20 25 30 35 y
LATERAL DISTANCE FROM THE TRACK CENTER = y-y_0 (μm)

Fig.5

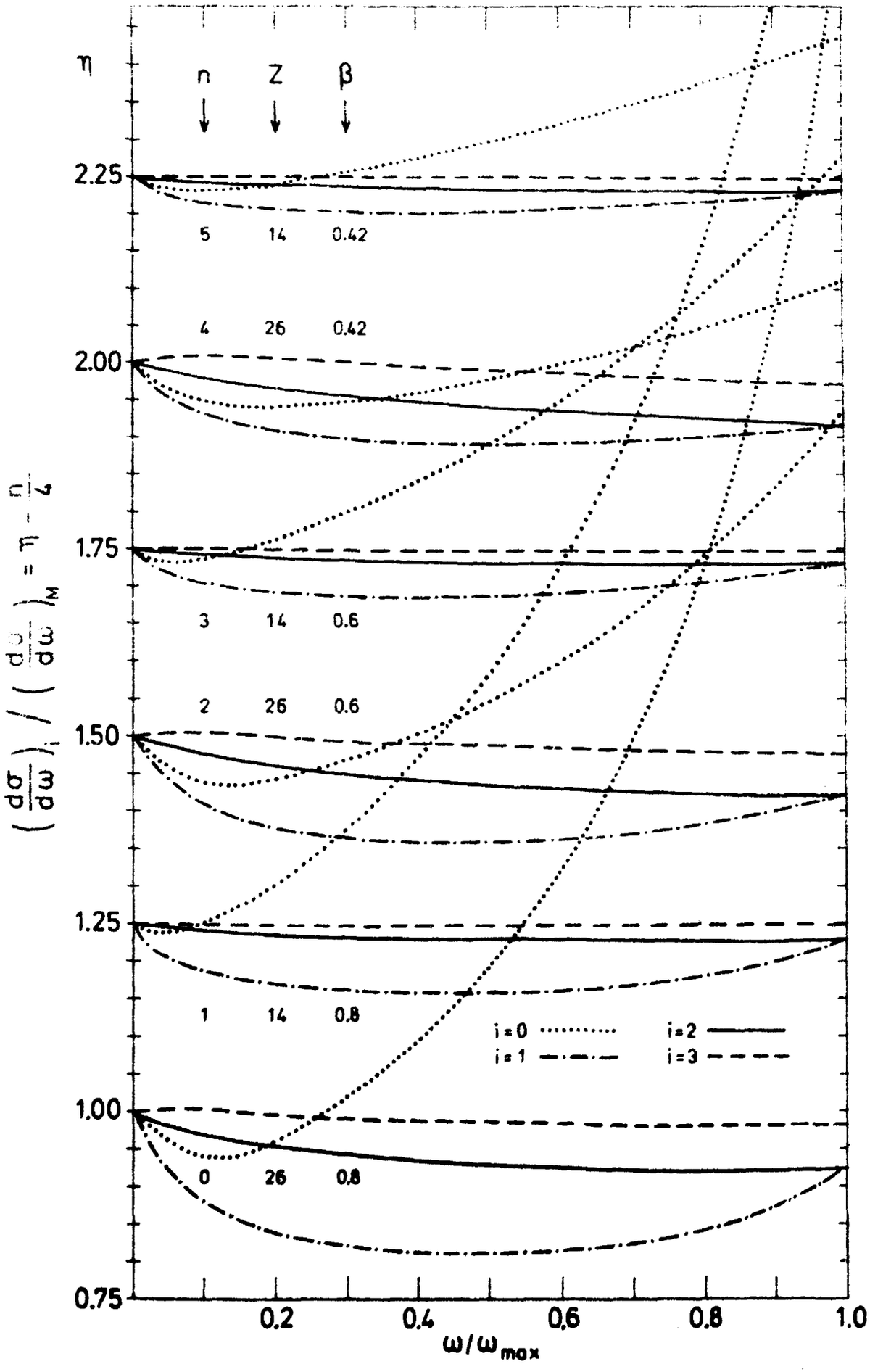
η
n Z β
2.25
2.00
1.75
1.50
1.25
1.00
0.75
5 14 0.42
4 26 0.42
3 14 0.6
2 26 0.6
1 14 0.8
0 26 0.8
i=0
i=1
i=2
i=3
0.2
0.4
0.6
0.8
1.0
ω/ω max
(dσ/dω)_i / (dσ/dω)_M = η - n/4

Fig.6

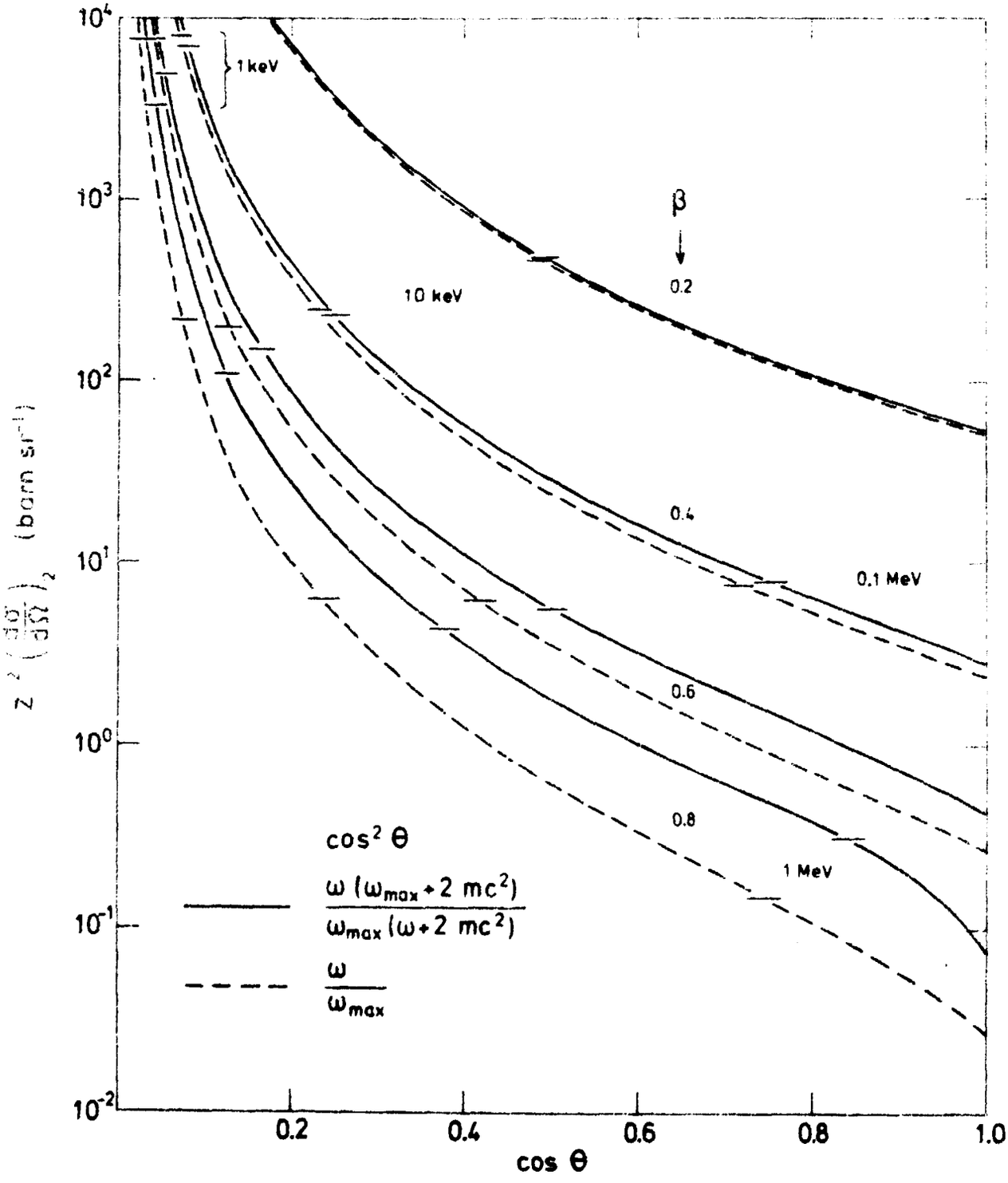
1 keV
10 keV
β
0.2
0.4
0.6
0.8
0.1 MeV
1 MeV
cos² θ
ω (ωmax + 2 mc²) / ωmax (ω + 2 mc²)
ω / ωmax
cos θ
Z² (dσ/dΩ)₂ (barn sr⁻¹)

Fig. 7